frontiers | Frontiers in Marine Science

TYPE Original Research
PUBLISHED 04 January 2024
DOI 10.3389/fmars.2023.1308689

OPEN ACCESS

EDITED BY
Timothy Jickells,
University of East Anglia, United Kingdom

REVIEWED BY
Neil Wyatt,
University of Plymouth, United Kingdom
Ashwini Kumar,
Council of Scientific and Industrial Research (CSIR), India

*CORRESPONDENCE
Cassandra J. Gaston
cgaston@miami.edu

RECEIVED 06 October 2023
ACCEPTED 14 December 2023
PUBLISHED 04 January 2024

CITATION
Elliott HE, Popendorf KJ, Blades E, Royer HM, Pollier CGL, Oehlert AM, Kukkadapu R, Ault A and Gaston CJ (2024) Godzilla mineral dust and La Soufrière volcanic ash fallout immediately stimulate marine microbial phosphate uptake.
Front. Mar. Sci. 10:1308689.
doi: 10.3389/fmars.2023.1308689

Godzilla mineral dust and La Soufrière volcanic ash fallout immediately stimulate marine microbial phosphate uptake

Hope Elizabeth Elliott[1], Kimberly J. Popendorf[1], Edmund Blades[1], Haley M. Royer[1], Clément G. L. Pollier[1], Amanda M. Oehlert[1], Ravi Kukkadapu[2], Andrew Ault[3] and Cassandra J. Gaston[1]*

[1]Rosenstiel School of Marine, Atmospheric & Earth Science, University of Miami, Miami, FL, United States, [2]Pacific Northwest National Laboratory, Richland, WA, United States, [3]Department of Chemistry, University of Michigan, Ann Arbor, MI, United States

During the "Godzilla" dust storm of June 2020, unusually high fluxes of mineral dust traveled across the Atlantic from the Sahara Desert, reaching the Caribbean Basin, Gulf Coast, and southeastern United States. Additionally, an eruption of the La Soufrière volcano on St. Vincent in April 2021 generated substantial ashfall in the southeastern Caribbean. While many studies have analyzed mineral dust's ability to relieve nutrient limitation of phosphorus (P) in the P-stressed North Atlantic, less is known about the impact of extreme events and other natural aerosols on fluxes of P into seawater and from seawater into marine microbial cells. We quantified P and iron (Fe) content in mineral dust from the Godzilla dust storm and volcanic ash from the La Soufrière eruption collected at Ragged Point, Barbados. We also performed seawater incubations to assess the marine microbial response to aerosol deposition. Using environmentally-relevant concentrations of atmospheric particles for within the ocean's mixed layer allowed us to draw realistic conclusions about how these deposition events impacted P cycling in situ. Volcanic ash has lower P content than mineral dust, and P in volcanic ash is far less soluble (~1%) than assumed in current atmospheric deposition models. Adding mineral dust and the volcanic ash leachate in concentrations representing different deposition scenarios increased soluble reactive phosphorus (SRP) concentrations in coastal seawater by ~7-32 nM. Phosphate uptake rate was stimulated in coastal seawater after either mineral dust or volcanic ash deposition at aerosol concentrations relevant to the Godzilla dust event, with ash eliciting the fastest uptake rate. Furthermore, high concentrations of both the mineral dust and volcanic ash led to slightly elevated alkaline phosphatase activity (APA) compared to the relevant controls, indicating higher potential for use of dissolved organic phosphorus (DOP) as a P source. Quantifying these aerosols' impacts on P cycling is a significant step towards achieving a better understanding of their potential roles in relieving nutrient limitation and fueling the biological carbon pump.

KEYWORDS

Saharan dust, volcano, deposition, phosphorus, biogeochemical

1 Introduction

Low phosphorus (P) concentrations documented in the subtropical Atlantic warrant further study of P inputs to this region (Ammerman et al., 2003 and references within; Mills et al., 2004; Lomas et al., 2010; Moore et al., 2013). Elevated nitrogen (N)-to-P ratios in dissolved and particulate organic and inorganic matter pools in near-surface waters of the northwestern subtropical Atlantic are indicative of P deficiency, and soluble reactive phosphorus (SRP) concentrations in surface waters at the Bermuda Atlantic Time Series (BATS) station are so low that they approach concentrations documented in the P-starved eastern Mediterranean (Ammerman et al., 2003 and references within; Lomas et al., 2010). Recent research has shown that mineral dust deposition to marine environments can relieve P stress by releasing phosphate, but little is known about how other natural aerosols impact marine P cycling (Mills et al., 2004; Zamora et al., 2013). Nutrient deposition caused by ashfall from volcanic eruptions, for example, has been implicated in a number of phytoplankton blooms throughout geologic history—but whether volcanic ash-derived P plays a role in stimulating phytoplankton growth in the modern, P-stressed North Atlantic remains uncertain (Sarmiento, 1993; Bains et al., 2000; Jicha et al., 2009; Langmann et al., 2010).

The magnitude of the soluble, and potentially bioavailable, P flux from volcanic ash into seawater is poorly understood, partially because studies of nutrient solubility in ash are complicated by the use of different leaching protocols and unrealistic aerosol:seawater ratios. Furthermore, many incubations meant to mimic aerosol deposition into seawater use soils or other proxies that may not be truly representative of airborne material subject to atmospheric deposition (Mills et al., 2004; Guieu et al., 2010; Guieu et al., 2014; Geisen et al., 2022). Without viable constraints on solubility, atmospheric deposition models often assume that P in volcanic ash is 100% soluble (Mahowald et al., 2008; Myriokefalitakis et al., 2016; Kanakidou et al., 2018 and references within), but this is likely an overestimate based on the reported P solubilities for other silica-based geological materials like mineral dust (often ~5-20%; Zamora et al., 2013; Barkley et al., 2019). The magnitude of the subsequent flux of volcanic ash-derived P from seawater into marine microbial cells after deposition is also unknown because ash's impacts on P uptake rate have never been experimentally measured.

Two major aerosol deposition events that impacted the Caribbean Basin and subtropical North Atlantic during the span of one year provide a unique opportunity to compare the effects of mineral dust and volcanic ash on P cycling in this region. In June 2020, mineral dust accumulated in coastal Africa due to a closed atmospheric circulation system associated with a strong North Atlantic subtropical high (NASH; Yu et al., 2021). The resulting dust plume, nicknamed "Godzilla," was carried to the Caribbean by the African easterly jet (AEJ; Yu et al., 2021). MODIS Terra records indicate that this event resulted in the highest aerosol optical depths (AODs) observed off the coast of North Africa and in the southeastern Caribbean Basin since 2000 (Yu et al., 2021). It was also a hazardous air quality event, with the PM_{10} concentration reaching 453 μg/m^3 in Cataño, Puerto Rico on June 23 (Yu et al., 2021). Then, in April 2021, an eruption of the La Soufrière volcano on St. Vincent—its first major explosive eruption since 1979—blanketed the Caribbean and northwestern subtropical Atlantic in volcanic ash. Collection of Godzilla mineral dust and La Soufrière volcanic ash transported to Ragged Point, Barbados, enabled us to use particles from both events collected after airborne transport for our measurements and bioassay incubation experiments.

We added nutrients leached from Godzilla mineral dust and La Soufrière volcanic ash to coastal seawater under laboratory conditions to evaluate how these aerosols impact P uptake into marine microbial cells. Phytoplankton can assimilate and use P in the form of inorganic phosphate without altering it, making dissolved inorganic phosphorus (DIP) the most "bioavailable" form of P for marine microbes (Mahaffey et al., 2014). Dissolved organic phosphorus (DOP) can also be utilized, but most commonly only if phosphate is released via hydrolysis mediated by enzymes like alkaline phosphatase (ALP) with specific metal requirements, making DOP less energetically favorable as a P source (Cembella et al., 1984; Chróst, 1991; Dyhrman and Ruttenberg, 2006; Twining and Baines, 2013 and references within). In our seawater incubations, we measured phosphate uptake rates using radiolabeled phosphate, and measured the rate at which phosphate is released from DOP using alkaline phosphatase activity (APA) quantified by fluorometry.

Our concurrent collection of soluble reactive phosphorus (SRP, an estimate of DIP), phosphate uptake rate, and APA measurements during a four-day bioassay incubation provided quantitative estimates of P fluxes from dust and volcanic ash aerosol into seawater and from seawater into marine microbial cells. While volcanic ash contains less P than in mineral dust, incubation data revealed that mineral dust and volcanic ash both have measurable impacts on phosphate uptake that vary depending on aerosol concentration.

2 Materials and methods

For our analysis, both mineral dust from the Godzilla dust storm and volcanic ash from the eruption of La Soufrière were collected at University of Miami's Barbados Atmospheric Chemistry Observatory at Ragged Point in eastern Barbados (13° 6′N, 59°37′W; see SI section 1. Dust mass concentrations measured at this site have documented African dust transport to the Caribbean and the Americas for over 50 years (Prospero et al., 2021). The site is also <200 km east of the La Soufrière volcano (13° 20′ N, 61°11′W) on St. Vincent and was impacted by ash fallout during its eruption in 2021. We coupled chemical analysis of the mineral dust and volcanic ash aerosols collected at this site with a seawater incubation to better constrain how the two major deposition events impacted marine P cycling.

2.1 Aerosol collection and dust mass measurements

Aerosol samples representative of mineral dust deposition during the Godzilla dust storm were collected in June 2020 on Whatman-41 (W-41) cellulose filters using a hi-volume aerosol sampler (average daily flow rate between 38 and 41 m^3/hr) atop a 17-meter tower at the

Ragged Point site, which sits on a 30 m high bluff. One-quarter filter portions were used to calculate dust mass concentrations in air. We washed the filters with 20 mL of 18 MΩ·cm MilliQ (ultrapure) water to remove soluble constituents and then followed the ashing procedure described in Prospero (1999) and Zuidema et al. (2019) to eliminate the filter component. A correction factor of 1.3 (see Zuidema et al., 2019) was applied to convert ash weight to mineral dust weight on the filters by accounting for the loss of soluble and volatile components. A procedural blank was collected by placing a filter in the sampling cassette with no vacuum applied under a laminar flow hood for 15 minutes and was then subjected to the same ashing procedure. Dust mass concentration reaching the collection site per volume of air pulled by the pump across the filter was determined using the pump air flow and sampling time. During the period between June 21st and June 24th, mineral dust mass concentrations at the Ragged Point site in Barbados (daily averages of 97.4-185.3 μg dust/m^3 air) were more than triple the typical concentrations (~30 μg dust/m^3 air) observed at the site during June (Prospero et al., 2012; Prospero, 2014; Zuidema et al., 2019; Figure 1). Volcanic ash samples from the La Soufrière eruption were collected from the Ragged Point site after the eruption blanketed eastern Barbados in ash in April 2021 (loose ash was collected from the top of a cellulose filter after deposition rather than contained within the matrix of a cellulose filter). Volcanic ash samples used for the incubation were stored at -20°C before use.

2.2 Determination of total P and Fe concentrations in dust and ash

One-eighth of a mineral dust filter collected during the Godzilla dust storm and a procedural blank filter were ashed overnight at 500°C to eliminate the filter component for elemental analysis. The ashed dust sample, procedural blank, and ~20 milligrams of volcanic ash sample were added to separate pre-cleaned 6 mL Savillex vials then digested at 150°C using a tri-acid cocktail (1 HNO_3: 3 HCl: 1 HF), evaporated to dryness, and resuspended in 6M distilled nitric acid (see Morton et al., 2013 for further information on aerosol digestion methods). A 0.5 mL aliquot of digested sample suspended in 6M nitric acid was diluted in 14.5 mL of 18 MΩ·cm MilliQ (ultrapure) water to approximate the matrix of the standards used to produce an external calibration curve. Elemental concentrations were determined using triple quadrupole inductively coupled plasma mass spectrometry (Agilent 8900 ICP-QQQ, Agilent, Santa Clara, CA), which has the advantage of being able to chemically resolve interferences using MS/MS mode with a variety of reaction cell/collision cell gases. For P measurements, the instrument was operated in MS/MS mode using O_2 gas in the collision-reaction cell (CRC) and analyzing the O_2 mass shifted analyte in the third quadrupole at mass 47. For Fe measurements, the instrument was operated in MS/MS mode using H_2 gas in the collision-reaction cell (CRC) and analyzing at mass 56. Multiple digestions of certified reference materials (CRMs), BHVO-2 and AGV-2, were used for method validation and estimates of accuracy in repeat analyses conducted during each analytical batch. Average recoveries for replicate measurements of each geostandard were within ±4% of the certified values for P and ±9% of the certified values for Fe. See SI section 2 for further detail on analytical methods and CRM recovery.

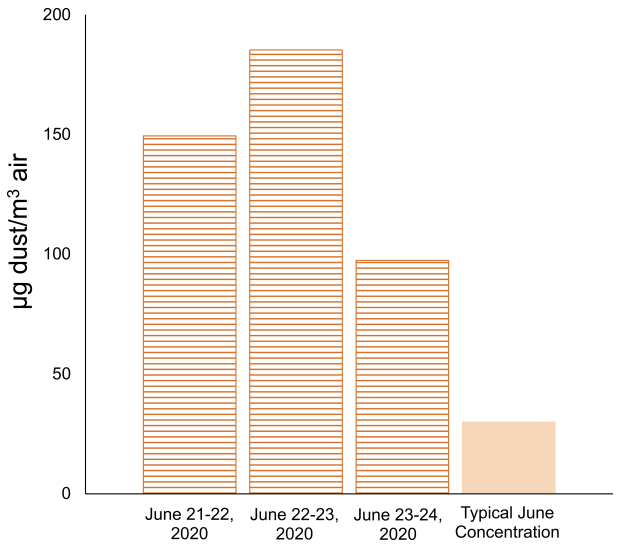

FIGURE 1
Daily average dust mass concentrations in air reaching Ragged Point, Barbados measured across three days during the Godzilla dust event, compared to approximate typical values for June based on Prospero et al. (2012), Prospero (2014), and Zuidema et al. (2019).

2.3 Mössbauer measurements

Mössbauer spectra were collected to characterize and quantify Feoxidation states and mineral forms present in both the mineral dust and volcanic ash samples. Mössbauer spectra were collected at the Pacific Northwest National Laboratory (PNNL) using a 75 mCi (initial strength) ^{57}Co/Rh source. The velocity transducer (WissEl Elektronik, Germany) was operated in a constant acceleration mode (23 Hz, ± 12 mm/sec). An Ar-Kr proportional counter was used to detect the radiation transmitted through the sample, and the counts were stored as a function of energy (transducer velocity, 1024 channels). Raw data were folded into 512 channels to give a flat background and a zero-velocity position corresponding to the center shift of a metal iron foil at 298 K (room temperature (RT)). Calibration spectra were obtained with a 7 μm thick α-Fe(m) foil (Amersham, England). A closed-cycle cryostat (SHI-850, Janis Research Company, Inc., Wilmington, MA) coupled with a Sumitomo CKW He compressor unit (Allentown, Pennsylvania) was used for decreasing the temperature from RT to desired below RT temperature.

2.4 Preliminary P solubility tests for volcanic ash

Prior to the incubation, batch leaching experiments were performed to better constrain P solubility for the volcanic ash specifically. Solubility was determined by leaching volcanic ash in

65 mL of 2.5 mM sodium bicarbonate (pH~8) in replicate 125 mL acid clean transparent polycarbonate bottles at a concentration of ~0.3 mg ash/mL. Leaching with this type of buffered solution is a staple in the atmospheric community (Baker et al., 2003; Baker et al., 2006). This specific solvent was selected to approximate seawater pH and buffer pH changes during the leach, following Aminot and Andrieux (1996) and Zamora et al. (2013). Over a 17-hour period, one bottle's leach was terminated each hour with filtration (syringe filtered through a 0.2 µm poresize polyethersulfone membrane) to remove ash particles, and leachate was frozen at -20°C until analysis. We quantified soluble phosphorus in the leachate both as SRP and total dissolved phosphorus (TDP = DIP + DOP).

2.4.1 Soluble reactive P in volcanic ash leachate

We added 2.5 M magnesium chloride to leachate samples to achieve a concentration of ~0.05 mol Mg^{2+}/L (comparable to typical seawater concentrations). SRP levels then were measured via the magnesium-induced co-precipitation (MAGIC) method (Murphy and Riley, 1962; Strickland and Parsons, 1972; Karl and Tien, 1992). Briefly, 10 mL of sample was precipitated as magnesium hydroxide using addition of sodium hydroxide. Pellets of precipitated magnesium hydroxide and phosphate were dissolved in 4 mL 0.25 M trace metal grade hydrochloric acid. The arsenate reduction correction was used (Johnson, 1971) prior to addition of molybdenum blue reagents (Strickland and Parsons, 1972) to eliminate possible interference with the determination of phosphate concentration. Absorbance of the samples was measured at 880 nm in a 10 cm quartz cuvette using a UV-1800 Shimadzu UV Spectrophotometer. Standards of potassium monobasic phosphate ranging from 0 nM to 150 nM were prepared in 2.5 mM sodium bicarbonate solution and processed in the same way as the samples.

2.4.2 Total dissolved P in volcanic ash leachate

For ICP-QQQ analysis, 5-mL leachate samples were acidified with 100 µL concentrated OmniTrace Ultra Nitric Acid to approximate the matrix of the calibration curve. TDP concentrations in leachate were determined using an Agilent 8900 ICP-QQQ as described above. Accuracy was assessed with NIST-traceable inorganic reference standards, and recovery for P was within ±8.5% (see SI section 3 for further detail on analytical methods and reference standard recovery).

2.5 Seawater bioassay incubation

For the incubation, mineral dust-laden filters and volcanic ash were leached in 2.5 mM sodium bicarbonate solution in acid clean transparent polycarbonate bottles at a concentration of ~0.48 g aerosol/L for 17 hours to extract soluble nutrients. Leaches were terminated with filtration using 0.2 µm polyethersulfone membrane syringe filters (Mackey et al., 2012; Zamora et al., 2013). Seawater was collected in coastal Miami (25°44′ N, 80°10′W) from the dock at the Rosenstiel School of Marine, Atmospheric, and Earth Science, where SRP concentrations have been measured ranging from approximately 20-200 nM. Seawater was collected in September 2022 using acid cleaned, high density polyethylene (HDPE) bottles dipped just below the surface in about 3 m deep water. Whole seawater was poured through a 250 µm nylon mesh to remove large particulate material. Mesh-filtered seawater was sampled for t=0 baseline seawater measurements. Leachate was diluted in coastal seawater collected at the dock to mimic four environmental deposition scenarios assuming an aerosol dry deposition velocity of 1.16 cm/s and a 20-m mixed layer depth (Duce et al., 1991; de Boyer Montégut et al., 2004; Mackey et al., 2012; Buck et al., 2013; see Table 1 for the concentrations used and rationale for the different conditions).

All dilutions of leachate into seawater resulted in a final concentration of 5% (v/v) 2.5 mM sodium bicarbonate in incubation solutions. We used lower aerosol concentrations compared to previous studies (Duggen et al., 2010 and references within; Geisen et al., 2022) in order to mimic environmentally realistic concentrations in the mixed layer. The "Godzilla Dust" and "La Soufrière Ash" conditions used the same mass of aerosol leached per volume seawater (0.0217 mg/L), so differences in observed outcomes were purely due to chemical differences of the aerosols. The "June Dust" condition (0.00451 mg/L) represented typical dust loading in June in the absence of a major event like Godzilla. The "High Deposition Ash" scenario (21.7 mg/L) represented higher loading of volcanic material. A "Blank Filter Control" produced by leaching a procedural blank cellulose filter was used as a control for the experimental conditions with mineral dust. A "Bicarbonate Control" with only the bicarbonate solution added to the seawater instead of aerosol leachate was used as an experimental control for the volcanic ash conditions.

Seawater was mixed with appropriate volumes of leachate or control solution in 2.5 L acid clean polycarbonate bottles, and triplicate time zero (t=0) samples were removed for SRP, phosphate uptake rate, APA, and cell count measurements on day 1 (t=0). The remaining incubation solution for each condition was then distributed into nine replicate 125 mL acid clean transparent polycarbonate bottles that were placed in flow-through incubators situated on the dock of the Rosenstiel School with ambient seawater circulating through them over four days. Incubators received ambient sunlight with neutral density screens filtering the light to approximate light levels at about 1 m depth. Temperature and light levels were monitored in the incubators throughout the course of the incubation using Onset HOBO MX2202 data loggers (see SI section 4). Three biological replicate bottles for each condition were removed from the incubators and sacrificed for sampling once per day on days 2-4 (t=1-3) for analysis in triplicate of the suite of measurements listed for t=0.

2.5.1 Seawater SRP

SRP samples were stored at -20°C until analysis. SRP was measured using the previously-described magnesium-induced co-precipitation (MAGIC) method (Murphy and Riley, 1962; Johnson, 1971; Strickland and Parsons, 1972; Karl and Tien, 1992), without the need to add magnesium chloride prior to precipitation. Standards were made using the SRP-free supernatant from coastal seawater samples with addition of potassium monobasic phosphate, then analyzed in the same way as the samples.

TABLE 1 Experimental and control conditions used for the seawater incubation.

Condition Name	Aerosol	Concentration	Description
Godzilla Dust	Godzilla mineral dust	0.0217 mg/L	Estimated aerosol concentration in the mixed layer during the Godzilla dust storm based on calculations of mineral dust mass collected at Ragged Point and a 3-day deposition event length based on Pu and Jin (2021)
La Soufrière Ash	La Soufrière volcanic ash	0.0217 mg/L	To match the concentration during the Godzilla dust storm
June Dust	Godzilla mineral dust	0.00451 mg/L	A more typical average concentration of mineral dust in the mixed layer for June, assuming a 30 $\mu g/m^3$ dust mass concentration in air at Ragged Point (Prospero et al., 2012; Prospero, 2014; Zuidema et al., 2019)
High Deposition Ash	La Soufrière volcanic ash	21.7 mg/L	Represents an extreme volcanic deposition scenario (1000 times the concentration used for the "La Soufrière Ash" condition)- also comparable to concentrations used in volcanic ash leaches and incubations in the literature (Duggen et al., 2010; Geisen et al., 2022)
Blank Filter Control	None	-	Control for the mineral dust experimental conditions, produced by leaching blank Whatman-41 filters
Bicarbonate Control	None	-	Control for the volcanic ash experimental conditions, made with 2.5 mM sodium bicarbonate

2.5.2 Phosphate uptake rate

Microbial phosphate uptake rate was measured directly after samples were collected from the dock at t=0 and immediately after bottles were collected from the incubators at t=1-3. From each 125 mL incubation bottle, a subsample of 20 mL was collected and spiked with 1 µCi radiolabeled orthophosphoric acid ($H_3{}^{32}PO_4$, Perkin Elmer NEX052001MC), resulting in a trace (pM) addition of phosphate (far below concentrations found in seawater and aerosol leachate). Killed controls were measured for each condition to distinguish biological phosphate uptake from potential abiotic adhesion to particles or the glass fiber filters. Water for killed controls was sampled from the original incubation bottles at t=0. Water totaling 20 mL pooled together was sampled from the three biological replicate bottles for killed controls at t=1 through t=3. Killed controls were treated with paraformaldehyde (PFA) at least 8 minutes prior to the radioisotope addition, with a final concentration of 0.5% (v/v) PFA, and then measured at timepoints alongside the samples. Within approximately 15 minutes of the radioisotope addition, 5 mL of sample or killed control was filtered through a combusted glass fiber membrane filter (GF-75, 0.3 µm pore size, 25 mm diameter) to capture cells and any radiolabeled phosphate they had taken up. From each radioisotope incubation vial, 5 mL samples were filtered at three timepoints across approximately 60 minutes. However, after evaluating the turnover time of the dissolved phosphate pool, only the first radioisotope incubation timepoint (within approximately 15 minutes of the spike) was used for calculation of phosphate uptake rates due to the rapid turnover rate of the dissolved phosphate pool. Filters were rinsed with 1 mL of filtered (0.2 µm) seawater, then transferred to a plastic scintillation vial and submerged in 3 mL Ultima Gold Scintillation cocktail. Total activity (TA) of the radioisotope addition was measured by drawing 100 µL from each replicate of radiolabeled incubation solution and adding to a scintillation vial with Ultima Gold scintillation cocktail. Radioactivity transferred to the GF-75 filters from the filtration rig were quantified using four filter blanks collected on day 1 (t=0) and day 4 (t=3). 5 mL of filtered 18 MΩ·cm MilliQ (ultrapure) water was passed through the filter blanks under the same conditions as samples, then submerging the filters in Ultima Gold Scintillation cocktail. ^{32}P activity was measured for filters and TA samples using a scintillation counter (Perkin Elmer Tri-Carb 2910 TR), measuring counts per minute (cpm) at 4-2000 keV; for high energy ^{32}P beta emission, 100% count efficiency is assumed such that cpm = decays per minute (dpm). The uptake rate of radioactivity into marine microbial cells (dpm/L/min) was calculated as the slope between sample activity and time since the radioactive spike, using the average radioactivity of the filter blanks collected at t=3 for activity at the time of the radioactive spike. Phosphate turnover time (turnover time of the dissolved phosphate pool) was calculated by dividing TA by uptake rate of radioactivity. Specific activity (SA, dpm/nmol P) was calculated by dividing TA by SRP. Phosphate uptake rate (nmol PO_4/L/hr) was calculated as slope (dpm/L/hr) divided by SA (see SI section 5 for details regarding calculations and SI section 6 for absolute phosphate turnover times).

2.5.3 APA

APA was measured after sampling at t=0, 2, and 3 using 4-methylumbelliferyl phosphate (MUF-P) fluorometry following the

method employed by Hoppe (1983). Both standards and samples were placed in a 96-well plate. Briefly, standards were made using 4-methylumbelliferone (MUB) in sterilized seawater, and MUF-P was added to triplicate samples to achieve a 25 µM concentration (appropriate concentration determined from prior experiments testing a range of substrate concentrations with coastal Miami seawater). Fluorescence measurements were collected 5-6 times within 2.2 hours of MUF-P addition using a Tecan Genios fluorescence plate reader. APA was quantified by calculating the increase in fluorescence as a slope over time (fluorescence/time since MUF-P addition) for each condition, then dividing by the standard curve slope (fluorescence/µM P) (see SI section 7 for details regarding calculations).

2.5.4 Cell counts

At each sampling timepoint, 1.5-mL samples for cell counts were fixed with PFA (0.5% final concentration), flash-frozen in a liquid nitrogen dewar, and stored at -80°C until analysis. Cell counts were determined using a BD Accuri C6 Plus Flow Cytometer, both with and without a SYBR Green I Nucleic Acid Stain (~0.5% of total sample volume, Lonza #50513). Phytoplankton were distinguished in unstained samples using forward scatter and chlorophyll fluorescence (488 nm excitation with 670 nm long-pass filter emission). Total cells were distinguished in stained samples using forward scatter and SYBR fluorescence (488 nm excitation with 533 nm ± 15 nm emission). Bacterial counts were determined by subtracting phytoplankton counts from total cell counts.

2.5.5 Statistical tests

Significance tests were performed with SRP concentration, phosphate uptake rate, phosphate turnover time, and APA rate data from the incubation by calculating the two-sample *t* statistic to compare experimental datapoints to values for the relevant controls at each timepoint and experimental values to their values at adjacent timepoints for the same condition. Matlab's student's *t* cumulative distribution function (tcdf) was used to compute 2-sided p-values from the absolute values of calculated *t* statistics. Significance was defined at the p=0.1 level.

3 Results

3.1 Volcanic ash and mineral dust chemical composition

P content in mineral dust (857 mg/kg) collected during the Godzilla dust storm is ~1.5× that of the P content La Soufrière volcanic ash (586 mg/kg; Figure 2). Fe content among the two aerosol types is more similar. Fe content in the volcanic ash (54,170 mg/kg) is only ~4% greater than the Fe content in the Godzilla dust (52,178 mg/kg), leading to an Fe:P ratio (wt/wt) of about 92.4 in the volcanic ash compared to 60.9 in the mineral dust. Mössbauer measurement also revealed key differences in mineralogy between the two aerosol types. Fe in the volcanic ash is primarily present as Fe(II), while Fe in the mineral dust is largely present as Fe(III) (Figure 3).

3.2 Solubility tests for volcanic ash

The solubility tests indicated that P solubility of volcanic ash in 2.5 mM $NaHCO_3$ is very low (~1%) (Figure 4). Additionally, most soluble P is released from the volcanic ash into solution within ~10 hours, and the amounts of DIP and TDP released are similar, implying that DOP release is negligible.

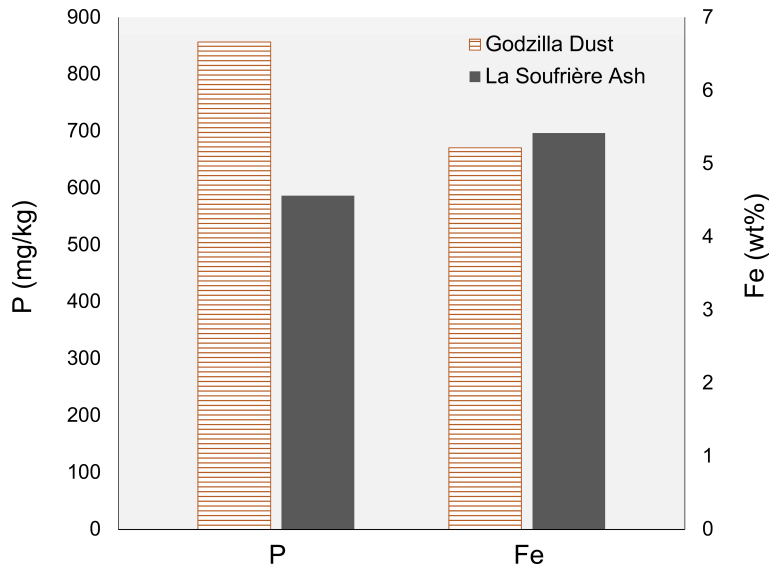

FIGURE 2
P and total Fe concentrations in Godzilla mineral dust and La Soufrière volcanic ash, determined by ICP-QQQ. Fe concentrations are much higher than P concentrations and are therefore reported as percents.

10.3389/fmars.2023.1308689

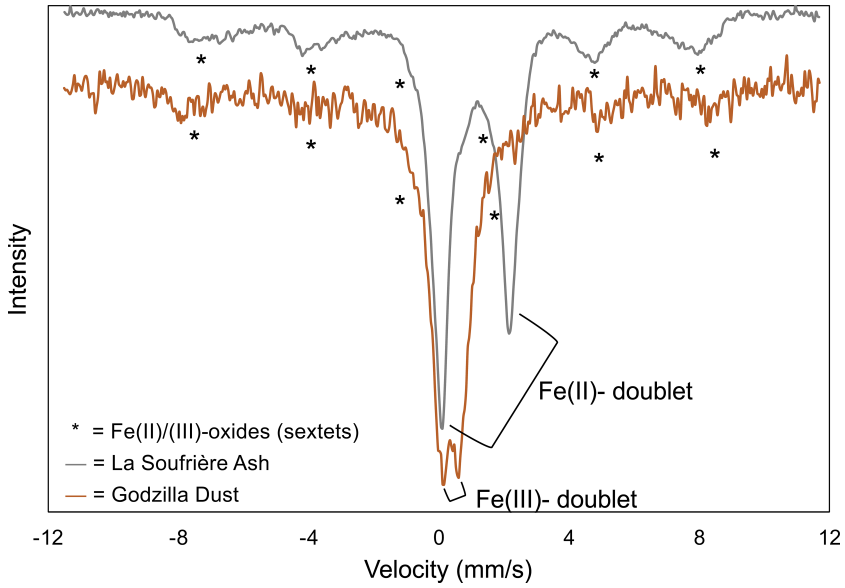

FIGURE 3
Room temperature Mössbauer spectra for Godzilla mineral dust (orange) and La Soufrière volcanic ash (grey).

3.3 Seawater bioassay incubation

While sampling occurred over four days, only data from the first three days (t=0-2) was utilized because of a spike in phytoplankton abundance at t=3 observed for all conditions and controls, likely due to a bottle effect (see SI section 8). Phytoplankton abundance significantly decreased over the first day and increased during the second day for all conditions (Figure 5). Heterotrophic bacteria abundance exhibited the opposite trend, but differences between t=0 and t=1 were not significant, and the change between t=1 and t=2 was only significant for the High Deposition Ash, Ash (Bicarbonate) Control, June Dust, and Dust (Filter) Control conditions.

Phosphate drawdown was evident over the course of the incubation (Figure 6). At t=0, SRP concentrations for all six conditions were significantly elevated above the background seawater SRP concentration at t=0, indicating that either the sodium bicarbonate or the leachate dilution process introduced a measurable background SRP concentration to the seawater. However, all four conditions with the addition of aerosol leachate had SRP concentrations significantly elevated over their relevant experimental controls at t=0, indicating that aerosol leachate added additional phosphate to the seawater. There was significant P drawdown for the La Soufrière Ash, High Deposition Ash, Ash (Bicarbonate) Control, Godzilla Dust, and June Dust between t=0 and t=1 but not for the Dust (Filter) Control. After 24 hours of

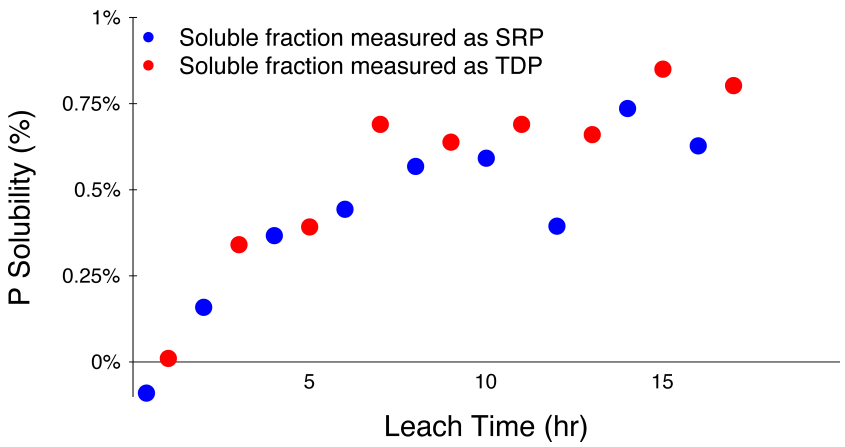

FIGURE 4
P solubility in La Soufrière volcanic ash as a function of leach time, represented as a percentage of total P content. Soluble P was assessed using two independent approaches: SRP measured using magnesium-induced co-precipitation, or MAGIC (blue circles), or TDP using ICP-QQQ (red circles).

10.3389/fmars.2023.1308689

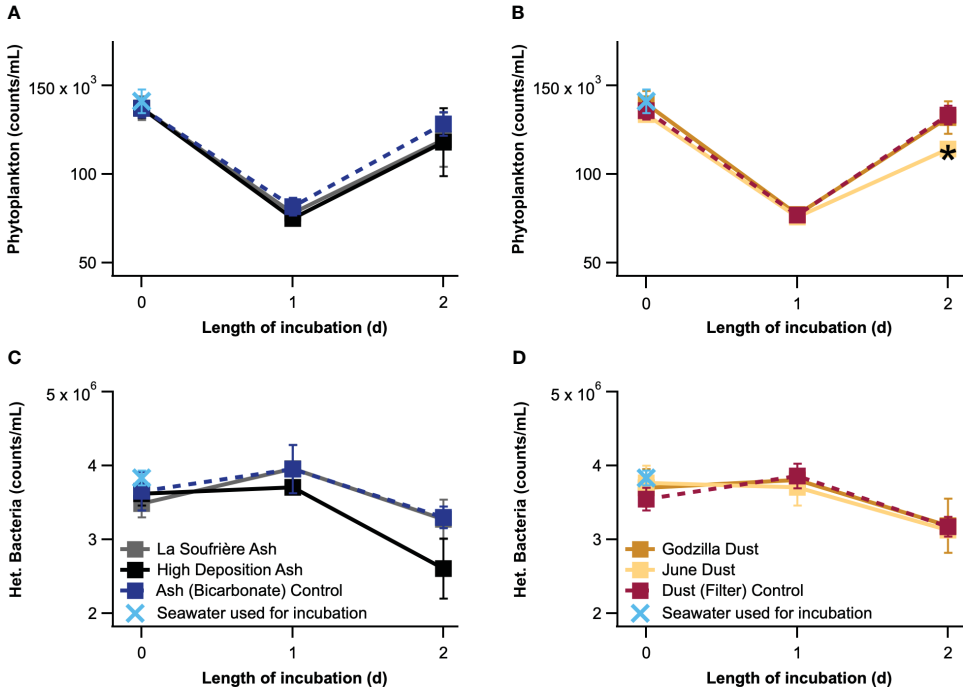

FIGURE 5
Phytoplankton **(A, B)** and heterotrophic bacteria **(C, D)** abundances measured for the four experimental conditions and two control conditions over three days. Error bars for phytoplankton abundance represent standard error, and error bars for heterotrophic bacteria represent propagated error. * indicates significant difference (p<0.1) from each timepoint's control.

incubation, at t=1, the High Deposition Ash, Godzilla Dust, and June Dust conditions had SRP concentrations significantly lower than their relevant controls. However, by t=1, phosphate concentrations had decreased in most bottles, such that between t=1 and t=2 further significant drawdown only occurred for the La Soufrière Ash, Ash (Bicarbonate) Control, and Dust (Filter) Control conditions. At t=2, only the Godzilla Dust experimental condition had SRP significantly elevated above its relevant control.

The most major impacts on microbial phosphate uptake rate were observed at t=0, immediately after adding aerosol leachate to the incubation bottles. At t=0, phosphate uptake rates were significantly elevated above rates for the relevant controls for all four experimental conditions, with the La Soufrière ash condition having the highest reported phosphate uptake rate overall (335.2 nmol phosphate/L/hr), despite having lower P content than the dust (Figure 6). By t=1, phosphate uptake rates for all experimental conditions and the Ash (Bicarbonate) Control had dropped significantly below their t=0 values (all <90 nmol phosphate/L/hr). At t=1, phosphate uptake rates were not significantly different from the relevant controls for any experimental condition (though it may be notable that the uptake rate for the High Deposition Ash condition was actually lower, though not significantly, than its control) (Figure 6). Uptake rates for all experimental conditions and controls increased significantly between t=1 and t=2. At t=2, only the Godzilla Dust condition (194.6 nmol phosphate/L/hr) had a phosphate uptake rate elevated significantly above its control.

Phosphate turnover time, which indicates the length of time that P remains in the dissolved phosphate pool before being taken up by marine microbes, is represented as a ratio to the relevant control at each timepoint in Figure 6 (see SI section 6 for a plot with absolute turnover times). Turnover times remained below 80 minutes throughout the incubation. While these are fast, the turnover times reported here are within the range of DIP turnover rates in coastal surface waters (typically from <1 hour to about 10 days) compiled by Ruttenberg (2001). At t=0, both the La Soufrière ash (28.0 min) and the High Deposition Ash (38.2 min) had significantly shorter turnover times than the Ash (Bicarbonate) Control (50.0 min). Similarly, both the Godzilla Dust (35.1 min) and June Dust (32.0 min) conditions had turnover times significantly shorter than that of the Dust (Filter) Control (65.5 min). Turnover times for all four experimental conditions (but neither control) significantly increased between t=0 and t=1, and turnover times for experimental conditions no longer significantly differed from those of the relevant controls at t=1. Turnover times significantly decreased between t=1 and t=2 for all experimental and control conditions, reflecting the low SRP levels and rebound in phosphate uptake rate at this timepoint. At t=2, all turnover times were faster than 35 minutes. The June Dust (20.5 min) had a significantly shorter turnover time than the Dust (Filter) Control (28.8 min), and the High Deposition Ash (23.9 min) had a significantly shorter turnover time than the Ash (Bicarbonate) Control (34.5 min) at t=2.

APA is reported for t=0 and t=2 (Figure 7). At t=0, APA was significantly elevated above the relevant controls for both of the volcanic ash conditions and the Godzilla Dust condition. The APA for the Godzilla Dust condition decreased significantly between t=0

10.3389/fmars.2023.1308689

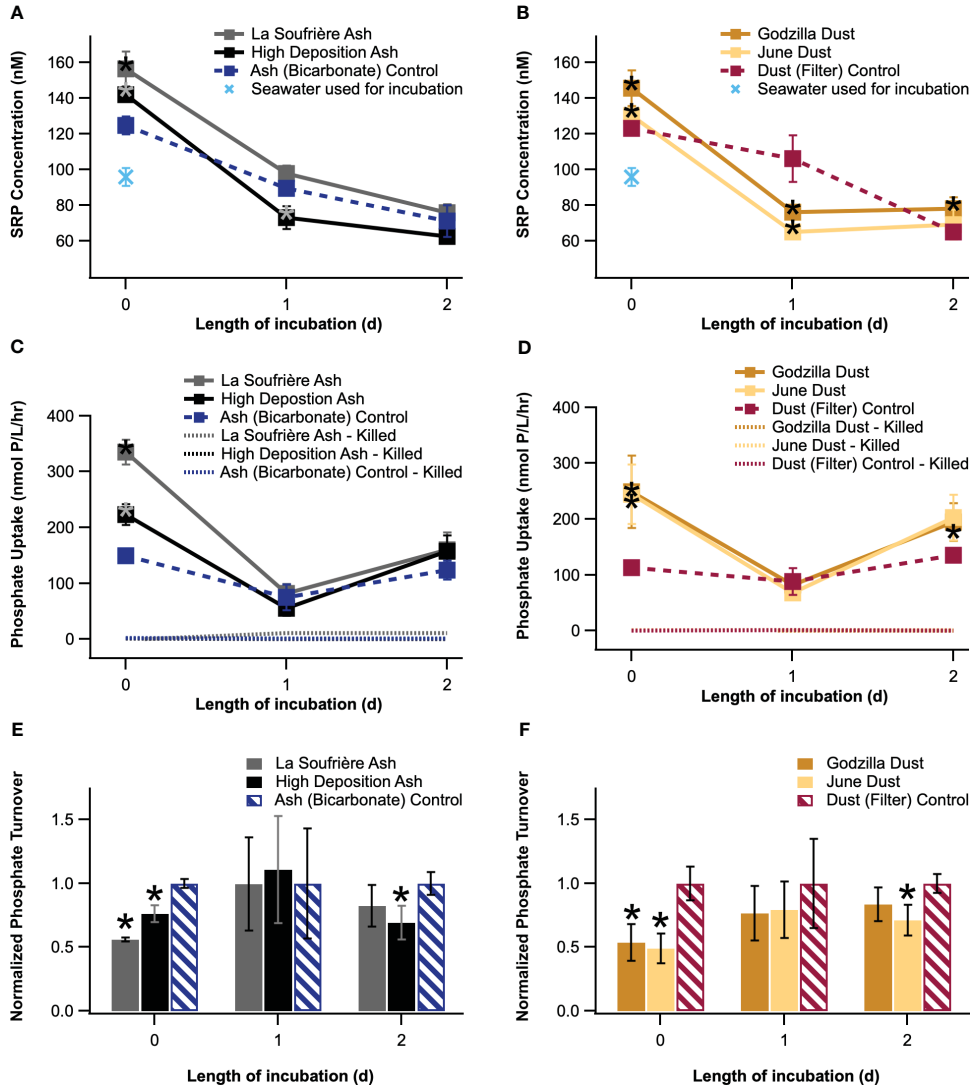

FIGURE 6
SRP concentration **(A, B)**, phosphate uptake rate **(C, D)**, and phosphate turnover time **(E, F)** measured for the four experimental conditions and two control conditions over three days. Phosphate uptake rate **(C, D)** is also reported for killed controls. Error bars represent standard error for replicate measurements in plots a and b and propagated error for plots c-f. * indicates significant difference (p<0.1) from each timepoint's control. (Note that significance was determined for turnover times before normalizing to the relevant controls.).

and t=2 (and increased significantly for its control). At t=2, while the APA rate for both volcanic ash conditions were elevated above the value reported for the Ash (Bicarbonate) Control, they were not significantly higher than the control due to the large variation between bottles.

4 Discussion

To the best of our knowledge, the data presented here are the first measurements of phosphate uptake rate, phosphate turnover time, and APA during a seawater bioassay incubation with volcanic ash. Adding La Soufrière ash resulted in a higher phosphate uptake rate than adding an identical amount of the mineral dust on an immediate timescale, despite ash's lower P content. Mineral dust, deposited in concentrations relevant to typical June conditions or during an extreme deposition event like the Godzilla dust storm, stimulated phosphate uptake into marine microbial cells on an immediate timescale. Our results, therefore, provide experimental evidence of mineral dust aerosol's ability to relieve P stress after long-range transport, as is hypothesized by Mills et al. (2004) based on experiments using surface soil. Notably, our results indicate only an immediate increase in phosphate uptake rate that did not persist throughout the duration of our incubation. By t=1, phosphate uptake rate was no longer significantly elevated above the controls for any of the experimental conditions, indicating that the leachate's immediate impact on phosphate uptake rate did not persist on a multi-day timescale. This result can at least partially be attributed to drawdown of SRP and lack of available phosphate in the incubation bottles by t=1. It may also reflect the fact that, while

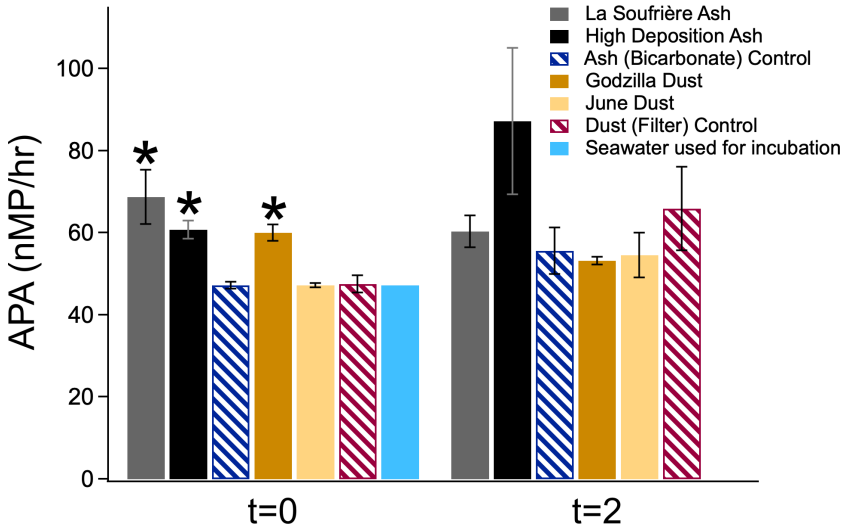

FIGURE 7
APA at the initial (t=0) and final (t=2) timepoints of the seawater incubation. Error bars represent standard error between the triplicate incubation bottles. * indicates significant difference (p<0.1) from each timepoint's control.

an immediate impact was observed, the leachate-derived SRP represents only a small portion of the daily microbial phosphate uptake and was utilized quickly.

Our results also provide evidence that major aerosol deposition events could have important biological impacts through the input of SRP into surface waters. By using realistic aerosol concentrations in our methodology, we produced reasonable estimates for SRP release into the mixed layer upon aerosol deposition for the La Soufrière eruption, Godzilla Dust storm, and similar future deposition events. We documented an increase of about 7.3 ± 3.8 nM SRP in seawater with the addition of mineral dust leachate at a concentration that is typical for the month of June. During the more extreme Godzilla Dust scenario, we measured an increase of about 22.4 ± 10.3 nM SRP compared to its control. Results for the La Soufrière Ash condition were comparable to the Godzilla Dust scenario, with an increase of 31.6 ± 11.0 nM SRP. While our study mimicked extreme deposition events occurring in a coastal environment with background SRP concentration of 95.7 ± 4.9 nM, the inputs of SRP documented here could have much more significant biological impacts in more oligotrophic, P-limited regions like the Sargasso Sea's euphotic zone where SRP levels are often <20 nM (Lomas et al., 2010).

We also compared P solubility of dust and ash to each other and to estimates currently used in biogeochemical models. Mineral dust is thought to be "processed" by mixing with reactive gases/acids or multiphase reactions in clouds during transit (Sullivan et al., 2007; Stockdale et al., 2016). Surface material on volcanic ash particles is subject to in-plume processing through rapid acid dissolution and interaction with water and liquid- and gas-phase fluoride that could potentially increase its nutrient solubility (Delmelle et al., 2007), but the percent solubility of P in the La Soufrière volcanic ash measured in our preliminary tests (<1%) was comparable to the solubility estimates obtained for mineral dust with our previous measurements (~1.44% for a 17.7-hour test leach) and other published studies (~5-20%; Zamora et al., 2013; Barkley et al., 2019). During our bioassay incubation experiment, t=0 SRP levels for the conditions in which equal concentrations of volcanic ash and mineral dust leachate were added to seawater were comparable, also indicating that volcanic ash solubility may in fact be close to mineral dust solubility (Figure 6). It should be noted that using the MAGIC method to measure SRP in sodium bicarbonate solution instead of seawater likely introduces some error. Since we have found that sodium bicarbonate introduces some level of background SRP signal, we do not recommend the use of sodium bicarbonate solution for leaches at low aerosol concentrations, despite its widespread use in the atmospheric community. Regardless, the 100% solubility estimates currently used for volcanic ash in atmospheric deposition models are likely an overestimate (Mahowald et al., 2008 and references within).

In addition to examining different facets of the marine phosphorus cycle, we also examined the impact on the marine microbial population. While leaching methodology varies significantly, both positive and negative impacts on marine microbes have been documented after interaction with volcanic ash in prior studies. Hoffmann et al. (2012) found that leachate produced using volcanic ash (0.53-1.6 g ash/L) from explosive eruptions of the Popocatepetl, Rabaul-Tavurvur, and Sakura-jima volcanoes increased the growth rate of a marine diatom (*Thalassiosira pseudonana*), while addition of leachate made using ash from the Arenal volcano decreased its growth rate. Adding leachate from the Popocatepetl, Rabaul-Tavurvur, and Arenal volcanoes appeared to have no significant impact on coccolithophore (*Emiliania huxleyi*) growth rates, but Sakura-jima ash leachate decreased this species' growth rate at concentrations corresponding to 0.53-2.67 g ash/L of seawater (Hoffmann et al., 2012). Zhang et al. (2017) leached volcanic ash from Iceland's Eyjafjallajökull volcano into filtered seawater from the western Pacific Ocean and found that the leachate reduced microbial

diversity and suppressed SAR11 bacteria's contribution to the microbial community structure. In the present study, total phytoplankton cell counts were not significantly different from controls 24 hours after addition of the mineral dust and volcanic ash, and only the June Dust condition varied significantly from its control after 48 hours. Since phosphate uptake rate was immediately stimulated with addition of the ash leachate but cell counts at subsequent timepoints were not significantly greater than those observed for the relevant control, it is possible that addition of the volcanic ash initially relieved P stress without causing an observable change in biomass. Alternatively, the input of SRP from the aerosol leachate may have enabled luxury P uptake (Solovchenko et al., 2019). We emphasize that the results presented here are likely more environmentally-relevant than those used for previous studies because we intentionally used concentrations of mineral dust and volcanic ash per volume seawater designed to mimic natural environmental deposition in the mixed layer. Chlorophyll-*a* concentrations will be measured in future studies to determine if biomass increases are associated with phosphate uptake rate because, overall, cell counts were not (Figure 5).

While our results have demonstrated that there is measurable phosphate release upon volcanic ash deposition into seawater, we speculate that the concurrent release of other nutrients including micronutrients may have also played an important role in the changes in phosphate uptake rate and APA that we observed. Since P was the major focus of our work, we used a leaching protocol that has been used in the atmospheric community for the analysis of SRP in aerosols (Baker et al., 2003; Baker et al., 2006). This protocol is not suitable for the accurate quantification of trace elements in our leachate. However, many studies have documented the release of other biologically important trace metals from ash during leaching experiments. Zhang et al. (2017) leached volcanic ash from Iceland's Eyjafjallajökull volcano into filtered seawater from the western Pacific Ocean and documented release of zinc (Zn), copper (Cu), lead (Pb), cobalt (Co), cadmium (Cd), and nickel (Ni). Similarly, Frogner et al. (2001) documented the release of significant amounts of manganese (Mn) upon dissolution of ash from the Hekla volcano in Iceland. Many of these trace elements play a documented role in controlling microbial cycling of phosphorus through their function in enzymes (Duhamel et al., 2021). It is, therefore, possible that P input alone is not totally responsible for the observed biological impacts of the volcanic material. Bioessential metals like Fe in the ash may have played a role in enhancing microbial phosphate uptake. Our Mössbauer measurements for mineral dust showed that Fe present in the dust is primarily Fe(III), which agrees with the analysis of sediment samples from north-central Africa by Moskowitz et al. (2016). Our volcanic ash has greater Fe content than the dust and contains more Fe(II) (Figure 2), which is thought to be more soluble and bioavailable than Fe(III) (Shaked and Lis, 2012). This finding agrees with results from Maters et al. (2017) that demonstrate dominance of Fe(II) over Fe(III) in bulk volcanic ash from the 2008 Chaitén, 2009 Redoubt, and 2010 Eyjafjallajökull eruptions. The elevated APA that we observed with addition of volcanic ash at t=0 also supports the potential biological importance of trace metals released from the ash (Figure 7). Higher APA rates are generally interpreted as a response to phosphate stress since hydrolyzing DOP is a strategy employed by marine microbes to obtain more bioavailable P (Dyhrman and Ruttenberg, 2006). While phosphate drawdown was observed, we hypothesize that, in this case, APA may be elevated for the High Deposition Ash condition partially due to large fluxes of biologically active metals from the ash (Jones and Gislason, 2008). Fe, Zn, and Co specifically may have led to enhanced APA and luxury P uptake due to the metal requirements of alkaline phosphatase enzymes (Twining and Baines, 2013, and references within). However, testing our hypothesis will require further analysis using different leaching methods appropriate for both P and trace micronutrients.

Compared to other aerosol inputs, far less is known about the impacts of volcanic ash on P cycling because eruptions are unpredictable. Our results show that both mineral dust and volcanic ash appear to cause short-term stimulation of phosphate uptake, but there is a need for standardization of leaching and incubation protocols so that the impacts of different types of volcanic material can be compared. In particular, the leaching protocols that are routinely used for quantifying SRP in aerosols complicate the analysis of trace metals in the resulting leachate. We speculate that essential micronutrients like Fe, rather than macronutrients alone, may be responsible for the impacts of both dust and volcanic ash on the flux of P into marine microbial cells. Testing the validity of our hypothesis will require a different leaching approach to more holistically measure the different micro and macro nutrients released upon contact with seawater. Quantifying nutrient release from natural aerosols specifically is important for climate modeling because natural emissions from dust and smoke are predicted to increase with the changing climate (Pechony and Shindell, 2010; Gomez et al., 2023). The impacts of climate change on volcanoes have not been extensively studied, but the importance of nutrient deposition from volcanic aerosol in even the modern climate remains uncertain (Aubry et al., 2022). The results presented in this study can help improve model estimates of P solubility for volcanic ash and quantitative estimates of SRP delivery upon deposition to the ocean surface. Our findings regarding the impacts of extreme deposition events like dust storms and volcanic eruptions on marine P cycling is a significant step towards achieving a better understanding of their impacts on primary productivity and, subsequently, carbon sequestration in the oceans.

Data availability statement

The raw data supporting the conclusions of this article will be made available by the authors, without undue reservation.

Author contributions

HE: Formal analysis, Investigation, Methodology, Validation, Writing – original draft, Writing – review & editing. KP: Conceptualization, Investigation, Methodology, Writing – review

& editing, Funding acquisition. EB: Resources, Writing – review & editing. HR: Investigation, Methodology, Writing – review & editing. CP: Investigation, Writing – review & editing. AO: Formal analysis, Investigation, Methodology, Writing – review & editing, Funding acquisition. RK: Formal analysis, Investigation, Writing – review & editing. AA: Funding acquisition, Writing – review & editing. CG: Conceptualization, Investigation, Methodology, Writing – review & editing, Funding acquisition.

Funding

The author(s) declare financial support was received for the research, authorship, and/or publication of this article. We acknowledge CJG's NSF CAREER award (AGS-1944958) and a user proposal (#51900) from the Environmental Molecular Sciences Laboratory at the Pacific Northwest National Laboratory sponsored by the Office of Biological and Environmental Research of the U.S. Department of Energy. HEE acknowledges the University of Miami Graduate School Dean's Fellowship. Start-up funds provided to AMO by the Rosenstiel School of Marine, Atmospheric, and Earth Science and Gaston's NSF CAREER award supported analyses conducted on the ICP-QQQ.

Acknowledgments

We thank the family of HC Manning and the Herbert C Manning Trust for providing access to their land. We thank the members of the Popendorf lab, including Daniela Maizel and Raquel Chenail, for assistance with the radioisotope incubations, and thank additional members of the Gaston lab, including James Christie, for assistance with APA and other timepoint measurements. We are grateful to Ali Pourmand and Arash Sharifi for laboratory assistance and access to equipment used for sample digestions. We thank two reviewers for their comments that improved this manuscript.

Conflict of interest

The authors declare that the research was conducted in the absence of any commercial or financial relationships that could be construed as a potential conflict of interest.

Publisher's note

All claims expressed in this article are solely those of the authors and do not necessarily represent those of their affiliated organizations, or those of the publisher, the editors and the reviewers. Any product that may be evaluated in this article, or claim that may be made by its manufacturer, is not guaranteed or endorsed by the publisher.

Supplementary material

The Supplementary Material for this article can be found online at: https://www.frontiersin.org/articles/10.3389/fmars.2023.1308689/full#supplementary-material

References

Aminot, A., and Andrieux, F. (1996). Concept and determination of exchangeable phosphate in aquatic sediments. *Water Res.* 30, 11. doi: 10.1016/S0043-1354(96)00192-3

Ammerman, J. W., Raleigh, R. H., Case, D. A., and Cotner, J. B. (2003). Phosphorus deficiency in the atlantic: an emerging paradigm in oceanography. *Eos* 84, 18. doi: 10.1029/2003EO180001

Aubry, T. J., Farquharson, J. I., Rowell, C. R., Watt, S. F. L., Pinel, V., Beckett, F., et al. (2022). Impact of climate change on volcanic processes: current understanding and future challenges. *Bull. Volcanology* 84, 6. doi: 10.1007/s00445-022-01562-8

Bains, S., Norris, R. D., Corfield, R. M., and Faul, K. L. (2000). Termination of global warmth at the Palaeocene/Eocene boundary through productivity feedback. *Nature* 407, 6801. doi: 10.1038/35025035

Baker, A. R., Jickells, T. D., Witt, M., and Linge, K. L. (2006). Trends in the solubility of iron, aluminum, manganese and phosphorus in aerosol collected over the Atlantic Ocean. *Mar. Chem.* 98, 1. doi: 10.1016/j.marchem.2005.06.004

Baker, A. R., Kelly, S. D., Biswas, K. F., Witt, M., and Jickells, T. D. (2003). Atmospheric deposition of nutrients to the Atlantic Ocean. *Geophysical Res. Lett.* 30, 24. doi: 10.1029/2003GL018518

Barkley, A. E., Prospero, J. M., Mahowald, N., Hamilton, D. S., Popendorf, K. J., Oehlert, A. M., et al. (2019). African biomass burning is a substantial source of phosphorus deposition to the Amazon, Tropical Atlantic Ocean, and Southern Ocean. *PNAS* 116, 33. doi: 10.1073/pnas.1906091116

Buck, C. S., Landing, W. M., and Resing, J. (2013). Pacific Ocean aerosols: Deposition and solubility of iron, aluminum, and other trace elements. *Mar. Chem.* 157, 117–130. doi: 10.1016/j.marchem.2013.09.005

Cembella, A. D., Antia, N. J., and Harrison, P. J. (1984). The utilization of inorganic and organic phosphorus compounds as nutrients by eukaryotic microalgae: A multidisciplinary perspective: Part 1. *CRC Crit. Rev. Microbiol.* 10, 4. doi: 10.3109/10408418209113567

Chróst, R. J. (1991). "Environmental control of the synthesis and activity of aquatic microbial ectoenzymes," in *Microbial Enzymes in Aquatic Environments*. Ed. R. J. Chróst (New York, NY: Springer-Verlag), 29–59.

de Boyer Montégut, C., Madec, G., Fischer, A. S., Lazar, A., and Iudicone, D. (2004). Mixed layer depth over the global ocean: An examination of profile data and a profile-based climatology. *J. Geophysical Res.* 109, C12003. doi: 10.1029/2004JC002378

Delmelle, P., Lambert, M., Dufrêne, Y., Gerin, P., and Óskarsson, N. (2007). Gas/aerosol–ash interaction in volcanic plumes: New insights from surface analyses of fine ash particles. *Earth Planetary Sci. Lett.* 259, 1–2. doi: 10.1016/j.epsl.2007.04.052

Duce, R. A., Liss, P. S., Merrill, J. T., Atlas, E. L., Buat-Menard, P., Hicks, B. B., et al. (1991). The atmospheric input of trace species to the world ocean. *Global Biogeochemical Cycles* 5, 3. doi: 10.1029/91GB01778

Duggen, S., Olgun, N., Croot, P., Hoffmann, L., Dietze, H., Delmelle, P., et al. (2010). The role of airborne volcanic ash for the surface ocean biogeochemical iron-cycle: a review. *Biogeosciences* 7, 3. doi: 10.5194/BG-7-827-2010

Duhamel, S., Diaz, J. M., Adams, J. C., Djaoudi, K., Steck, V., and Waggoner, E. M. (2021). Phosphorus as an integral component of global marine biogeochemistry. *Nat. Geosci.* 14, 6. doi: 10.1038/s41561-021-00755-8

Dyhrman, S. T., and Ruttenberg, K. C. (2006). Presence and regulation of alkaline phosphatase activity in eukaryotic phytoplankton from the coastal ocean: Implications for dissolved organic phosphorus remineralization. *Limnology Oceanography.* 51, 3. doi: 10.4319/lo.2006.51.3.1381

Frogner, P., Gíslason, S. R., and Óskarsson, N. (2001). Fertilizing potential of volcanic ash in ocean surface water. *Geology* 29, 6. doi: 10.1130/0091-7613(2001)029<0487:FPOVAI>2.0.CO;2

Geisen, C., Ridame, C., Journet, E., Delmelle, P., Marie, D., Lo Monaco, C., et al. (2022). Phytoplanktonic response to simulated volcanic and desert dust deposition events in the South Indian and Southern Oceans. *Limnology Oceanography* 67, 7. doi: 10.1002/lno.12100

Gomez, J., Allen, R. J., Turnock, S. T., Horowitz, L. W., Tsigaridis, K., Bauer, S. E., et al. (2023). The projected future degradation in air quality is caused by more abundant natural aerosols in a warmer world. *Commun. Earth Environ.* 4, 1. doi: 10.1038/s43247-023-00688-7

Guieu, C., Aumont, O., Paytan, A., Bopp, L., Law, C. S., Mahowald, N., et al. (2014). The significance of the episodic nature of atmospheric deposition to Low Nutrient Low Chlorophyll regions. *Global Biogeochemical Cycles* 28, 11. doi: 10.1002/2014GB004852

Guieu, C., Dulac, F., Desboeufs, K., Wagener, T., Pulido-Villena, E., Grisoni, J.-M., et al. (2010). Large clean mesocosms and simulated dust deposition: a new methodology to investigate responses of marine oligotrophic ecosystems to atmospheric inputs. *Biogeosciences* 7, 9. doi: 10.5194/bg-7-2765-2010

Hoffmann, L. J., Breitbarth, E., Ardelan, M. V., Duggen, S., Olgun, N., Hassellöv, M., et al. (2012). Influence of trace metal release from volcanic ash on growth of Thalassiosira pseudonana and Emiliania huxleyi. *Marine Chem.* 132–133, 28–33. doi: 10.1016/j.marchem.2012.02.003

Hoppe, H.-G. (1983). Significance of exoenzymatic activities in the ecology of brackish water: Measurements by means of methylumbelliferyl-substrates. *Mar. Ecol. Prog. Ser.* 11, 3. doi: 10.3354/meps011299

Jicha, B. R., Scholl, D. W., and Rea, D. K. (2009). Circum-Pacific arc flare-ups and global cooling near the Eocene-Oligocene boundary. *Geology* 37, 4. doi: 10.1130/G25392A.1

Johnson, D. L. (1971). Simultaneous determination of arsenate and phosphate in natural waters. *Environ. Sci. Technol.* 5, 5. doi: 10.1021/es60052a005

Jones, M. T., and Gislason, S. R. (2008). Rapid releases of metal salts and nutrients following the deposition of volcanic ash into aqueous environments. *Geochimica Cosmochimica Acta* 72, 15. doi: 10.1016/j.gca.2008.05.030

Kanakidou, M., Myriofalitakis, S., and Tsigaridis, K. (2018). Aerosols in atmospheric chemistry and biogeochemical cycles of nutrients. *Environ. Res. Lett.* 13, 6. doi: 10.1088/1748-9326/aabcdb

Karl, D. M., and Tien, G. (1992). MAGIC: A Sensitive and precise method for measuring dissolved phosphorus in aquatic environments. *Limnology Oceanography* 37, 1. doi: 10.4319/lo.1992.37.1.0105

Langmann, B., Zakšek, K., Hort, M., and Duggen, S. (2010). Volcanic ash as fertiliser for the surface ocean. *Atmospheric Chem. Phys.* 10, 8. doi: 10.5194/acp-10-3891-2010

Lomas, M. W., Burke, A. L., Lomas, D. A., Bell, D. W., Shen, C., Dyhrman, S. T., et al. (2010). Sargasso Sea phosphorus biogeochemistry: an important role for dissolved organic phosphorus (DOP). *Biogeosciences* 7, 2. doi: 10.5194/bg-7-695-2010

Mackey, K. R. M., Roberts, K., Lomas, M. W., Saito, M. A., Post, A. F., and Paytan, A. (2012). Enhanced solubility and ecological impact of atmospheric phosphorus deposition upon extended seawater exposure. *Environ. Sci. Technol.* 46, 19. doi: 10.1021/es3007996

Mahaffey, C., Reynolds, S., Davis, C. E., and Lohan, M. C. (2014). Alkaline phosphatase activity in the subtropical ocean: insights from nutrient, dust and trace metal addition experiments. *Front. Mar. Sci.* 1. doi: 10.3389/fmars.2014.00073

Mahowald, N., Jickells, T. D., Baker, A. R., Artaxo, P., Benitez-Nelson, C. R., Bergametti, G., et al. (2008). Global distribution of atmospheric phosphorus sources, concentrations and deposition rates, and anthropogenic impacts. *Global Biogeochemical Cycles* 22, 4. doi: 10.1029/2008GB003240

Maters, E. C., Delmelle, P., and Gunnlaugsson, H. P. (2017). Controls on iron mobilization from volcanic ash at low pH: Insights from dissolution experiments and Mössbauer spectroscopy. *Chem. Geology* 449, 73–81. doi: 10.1016/j.chemgeo.2016.11.036

Mills, M. M., Ridame, C., Davey, M., La Roche, J., and Geider, R. J. (2004). Iron and phosphorus co-limit nitrogen fixation in the eastern tropical North Atlantic. *Nature* 429, 6989. doi: 10.1038/nature02550

Moore, J. K., Lindsay, K., Doney, S. C., Long, M. C., and Misumi, K. (2013). Marine ecosystem dynamics and biogeochemical cycling in the community earth system model [CESM1(BGC)]: comparison of the 1990s with the 2090s under the RCP4.5 and RCP8.5 scenarios. *J. Climate* 26, 23. doi: 10.1175/JCLI-D-12-00566.1

Morton, P. L., Landing, W. M., Hsu, S.-C., Milne, A., Aguilar-Islas, A. M., Baker, A. R., et al. (2013). Methods for the sampling and analysis of marine aerosols: results from the 2008 GEOTRACES aerosol intercalibration experiment. *Limnology Oceanography: Methods* 11, 2. doi: 10.4319/lom.2013.11.62

Moskowitz, B. M., Reynolds, R. L., Goldstein, H. L., Berquó, T. S., Kokaly, R. F., and Bristow, C. S. (2016). Iron oxide minerals in dust-source sediments from the Bodélé Depression, Chad: Implications for radiative properties and Fe bioavailability of dust plumes from the Sahara. *Aeolian Res.* 22, 93–106. doi: 10.1016/j.aeolia.2016.07.001

Murphy, J., and Riley, J. P. (1962). A modified single solution method for the determination of phosphate in natural waters. *Analytica Chimica Acta* 27, 31–36. doi: 10.1016/S0003-2670(00)88444-5

Myriokefalitakis, S., Nenes, A., Baker, A. R., Mihalopoulos, N., and Kanakidou, M. (2016). Bioavailable atmospheric phosphorus supply to the global ocean: a 3-D global modelling study. *Biogeosciences* 13, 24. doi: 10.5194/bg-13-6519-2016

Pechony, O., and Shindell, D. T. (2010). Driving forces of global wildfires over the past millennium and the forthcoming century. *Proc. Natl. Acad. Sci.* 107, 45. doi: 10.1073/pnas.1003669107

Prospero, J. M. (1999). Long-term measurements of the transport of African mineral dust to the southeastern United States: Implications for regional air quality. *J. Geophysical Research: Atmospheres* 104, D13. doi: 10.1029/1999JD900072

Prospero, J. M. (2014). Characterizing the temporal and spatial variability of African dust over the Atlantic. *Past Global Changes* 22, 2. doi: 10.22498/pages.22.2.68

Prospero, J. M., Bullard, J. E., and Hodgkins, R. (2012). High-latitude dust over the north atlantic: inputs from Icelandic proglacial dust storms. *Science* 335, 6072. doi: 10.1126/science.1217447

Prospero, J. M., Delany, A. C., Delany, A. C., and Carlson, T. N. (2021). The discovery of african dust transport to the western hemisphere and the saharan air layer: A history. *Bull. Am. Meteorological Soc.* 102, 6. doi: 10.1175/BAMS-D-19-0309.1

Pu, B., and Jin, Q. (2021). A record-breaking trans-atlantic african dust plume associated with atmospheric circulation extremes in june 2020. *Bull. Am. Meteorological Soc.* 102, 7. doi: 10.1175/BAMS-D-21-0014.1

Ruttenberg, K. C. (2001). "Phosphorus cycle," in *Marine Chemistry and Geochemistry: A Derivative of Encyclopedia of Ocean Sciences, 2nd Edition*. Ed. K. K. Turekian (London: Academic Press), 567–579.

Sarmiento, J. L. (1993). Atmospheric CO_2 stalled. *Nature* 365, 6448. doi: 10.1038/365697a0

Shaked, Y., and Lis, H. (2012). Disassembling iron availability to phytoplankton. *Front. Microbiol.* 3. doi: 10.3389/fmicb.2012.00123

Solovchenko, A. E., Ismagulova, T. T., Lukyanov, A. A., Vasilieva, S. G., Konyukhov, I. V., Pogosyan, S. I., et al. (2019). Luxury phosphorus uptake in microalgae. *J. Appl. Phycology* 31, 5. doi: 10.1007/s10811-019-01831-8

Stockdale, A., Krom, M. D., Mortimer, R. J. G., Benning, L. G., Carslaw, K. S., Herbert, R. J., et al. (2016). Understanding the nature of atmospheric acid processing of mineral dusts in supplying bioavailable phosphorus to the oceans. *Proc. Natl. Acad. Sci.* 113, 51. doi: 10.1073/pnas.1608136113

Strickland, J. D. H., and Parsons, T. R. (1972). *A Practical Handbook of Seawater Analysis. 2nd ed* (Ottawa: Fisheries Research Board of Canada).

Sullivan, R. C., Guazzotti, S. A., Sodeman, D. A., and Prather, K. A. (2007). Direct observations of the atmospheric processing of Asian mineral dust. *Atmospheric Chem. Phys.* 7, 5. doi: 10.5194/acp-7-1213-2007

Twining, B. S., and Baines, S. B. (2013). The trace metal composition of marine phytoplankton. *Annu. Rev. Mar. Sci.* 5 (1), 191–215. doi: 10.1146/annurev-marine-121211-172322

Yu, H., Tan, Q., Zhou, L., Zhou, Y., Bian, H., Chin, M., et al. (2021). Observation and modeling of the historic "Godzilla" African dust intrusion into the Caribbean Basin and the southern US in June 2020. *Atmospheric Chem. Phys.* 21, 16. doi: 10.5194/acp-21-12359-2021

Zamora, L. M., Prospero, J. M., Hansell, D. A., and Trapp, J. M. (2013). Atmospheric P deposition to the subtropical North Atlantic: sources, properties, and relationship to N deposition. *J. Geophysical Research: Atmospheres* 118, 3. doi: 10.1002/jgrd.50187

Zhang, R., Jiang, T., Tian, Y., Xie, S., Zhou, L., Li, Q., et al. (2017). Volcanic ash stimulates growth of marine autotrophic and heterotrophic microorganisms. *Geology* 45, 8. doi: 10.1130/G38833.1

Zuidema, P., Alvarez, C., Kramer, S. J., Custals, L., Izaguirre, M., Sealy, P., et al. (2019). Is summer african dust arriving earlier to Barbados?: the updated long-term *in situ* dust mass concentration time series from ragged point, Barbados, and miami, florida. *Bull. Am. Meteorological Soc.* 100, 10. doi: 10.1175/BAMS-D-18-0083.1